7 Search for the rare decay $\mu^+ \to e^+e^-e^+$

R. Gredig, P. Robmann, and U. Straumann

in collaboration with: University of Geneva, Paul Scherrer Institute, ETH Zürich, University of Heidelberg, University of Mainz, Karlsruhe Institute of Technology

(Mu3e Collaboration)

Lepton flavor violation (LFV), as observed in neutrino oscillations, does not lead to measurable rates for LFV decays of charged leptons. Those would definitely be a clear signal for physics beyond the standard model. Mu3e plans to search for the decay $\mu \to e^+e^-e^+$ with a sensitivity at least three orders of magnitude beyond the present limit, set way back in the previous millennium by the SINDRUM I Collaboration [1] led by our institute. In the past years we have been working on the scintillating fibre tracker (see Fig. 7.1) and its readout and the results of these studies are presented below.

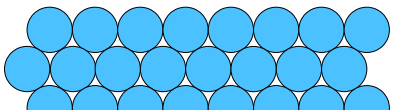

FIG. 7.1 – Cross-section through a scintillating-fibre ribbon.

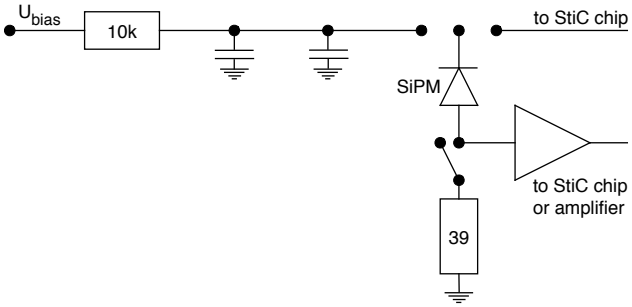

FIG. 7.2 – Electronic scheme of the sensor board. The wiring is repeated for each SiPM. The top switch is used to select a common bias voltage for single ended readout or an individual biasing for differential readout. In the differential readout case the signal goes to the amplifier before the shunt resistor and needs to be opened therefore.

[1] W. Bertl, S. Egli, R. Eichler, R. Engfer, L. Felawka, C. Grab, E.A. Hermes, N. Kraus, N. Lordong, J. Martino, H.S. Pruys, A. v.d. Schaaf and H.K. Walter, Nucl. Phys. B260 (1985) 1.

7.1 Improved SiPM Electronics

Figure 7.2 shows a simplified schematic of the read-out electronics focusing on the sensor-board. Pictures of the board are shown in Fig. 7.3. Two different ways are allowed to bias each SiPM. Either a common voltage is used that powers all the SiPMs with the same voltage or an individual voltage for each sensor can be applied. The voltage distribution uses a low-pass filter before each SiPM to decouple them electronically.

If used with the amplifier the readout is single ended over the shunt resistor. The readout with the STiC chip is done differential. In this case all the pre-amplification electronics is provided by the chip and the sensor-board only needs to connect the SiPM to the STiC.

7.2 Crosstalk Studies

Optical crosstalk between the fibres needs to be understood properly. The crosstalk not only worsens the time resolution but also increases the rate per channel.

Figure 7.4 shows a typical result of the crosstalk analysis. In this measurement the ribbon is irradiated in the middle with electrons from a ^{90}Sr source. Two layers are connected to the readout electronics. Events are selected in which in fibre a a signal is observed. The figure shows

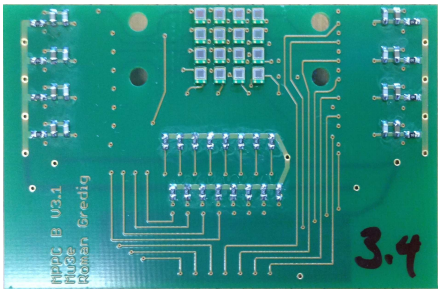

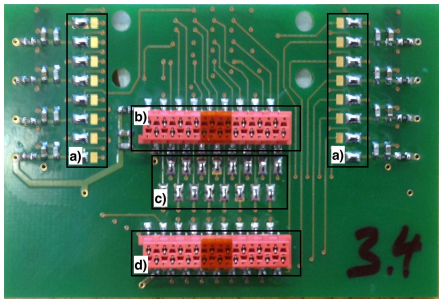

FIG. 7.3 – 3rd generation sensor board. The solder pads *a*) are used to change between common and individual high voltage from the STiC chip. The micro-match plug *b*) uses the same pin-out as the 2nd generation board. For use with the STiC chip the resistors to ground can be switched off with the solder-pads *c*) and the circuit connected to the STiC with *d*).

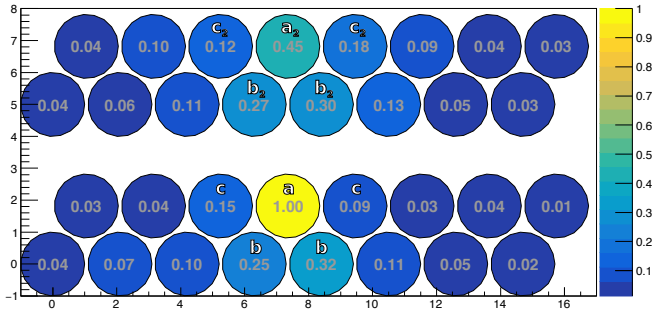

FIG. 7.4 – Result of our crosstalk studies with a ^{90}Sr source. The numbers in gray show the probability to observe a signal when there was a signal in fibre a. The upper and lower parts of the figure show the results from the two ends separately. See text for further details.

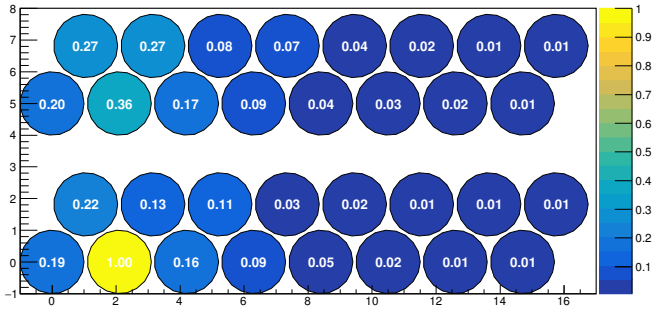

FIG. 7.5 – Crosstalk showing also some fake-crosstalk hits at the right side of the ribbon due to the high decay rate of the source used in the laboratory.

the probability of observing a signal in the other fibres too. The electrons crossing fibre a will also cross one of the fibres b (except when the particle crosses exactly in between them) which explains the observed high values for fibres b. The closest fibres for which crosstalk can be studied are fibres c. Those show crosstalk probabilities of up to 20 %.

Crosstalk depends on the position of the layer in the ribbon. Outside layers have neighbors on one side only. The inside layer has neighbors on both sides (cf. Fig. 7.1). The crosstalk probability for outside layers is on average (11 ± 3) %, for the inside layer we observe (18 ± 3) %. For the next neighbors the crosstalk is (8.3 ± 1.4) % and (5.0 ± 1.6) %, respectively.

Our crosstalk probabilities must be corrected for accidental coincidences which depend on signal rate and time window. With a typical dark-count rate of $1 \cdot 10^5$ counts per second above a 0.5 photo-electron threshold, a source rate of similar magnitude, and a time window of 20 ns the probability for accidental background is about $4 \cdot 10^{-3}$. For large distances this is the dominant contribution to the observed probabilities.

7.3 Detector efficiencies

The detection efficiency was measured with 160 MeV electrons at the PSI cyclotron. As illustrated in Fig. 7.6 the ribbon was oriented horizontally so a single beam electron could cross many fibres. The beam energy is more than sufficient to guarantee that the electron crosses all fibres and does not stop within the ribbon. The measuring principle for the different fibres is shown in Fig. 7.6 as well. The fibre under investigation is compared with its two nearest neighbors. The efficiency is defined as the probability to detect one photon in the middle fibre when the two neighboring fibres observe at least one photon each. Results are shown in Table 7.1 for each of the 24 fibres under investigation.

FIG. 7.6 – Principle of the efficiency measurement. For each fibre a cluster of three fibres is used (grey, yellow, red in this example) to specify the efficiency of the fibre in the middle of a cluster.

The results show that the fibre efficiency varies a lot between different channels for which we see two reasons. On the one hand there can be a large variety in the fibre quality caused by imperfections in the production process. Especially the extremely thin fibre cladding can be destroyed by improper handling. Also crazing, the production of micro cracks due to finger grease or sweat acids, can be a problem as the ribbons are manufactured manually. In this case the manufacturing procedures need to be improved. The second potential problem source is bad coupling of the fibres to the sensors. Especially in the case of single photon experiments a geometric misalignment, dirt or bad polishing can have strong influence

TAB. 7.1 – Single fibre efficiency eff defined as the probability of detecting a photon in the middle fibre when each of the two surrounding fibres observed a signal.

fibre	eff	fibre	eff	fibre	eff	fibre	eff
1	0.73	7	0.47	13	0.65	19	0.72
2	0.64	8	0.72	14	0.64	20	0.55
3	0.68	9	0.50	15	0.69	21	0.74
4	0.70	10	0.51	16	0.65	22	0.70
5	0.68	11	0.37	17	0.71	23	0.71
6	0.70	12	0.74	18	0.66	24	0.67

TAB. 7.2 –
Efficiencies for two fibres. The values show the probability of detecting a photon in one of the middle fibres (OR condition) when there is a photon detected in the two surrounding fibres.

pair	eff	pair	eff	pair	eff	pair	eff
1	0.87	6	0.82	11	0.84	16	0.83
2	0.84	7	0.84	12	0.85	17	0.85
3	0.86	8	0.72	13	0.84	18	0.90
4	0.86	9	0.66	14	0.86	19	0.89
5	0.87	10	0.82	15	0.86	20	0.87

on the efficiency. The use of optical grease has not been envisaged as the transparency of the grease tends to degrade in time. A better coupling would certainly be reached by glueing the fibres to the sensors. In this early R&D stage with only one ribbon available and different sensors to be tested glueing was, however, no option.

As the final experiment will have more than one layer of fibres the efficiencies for two and three layers have been estimated as well. In case of two layers new clusters including four fibres have been used for measuring the efficiency. The probability to observe at least one photon in one of the two middle fibres (OR) when the two outer fibres show at least one photon each defines the new efficiency. The measured results are shown in Table 7.2.

TAB. 7.3 –
Predicted double fibre efficiencies.

fibre	eff	fibre	eff	fibre	eff	fibre	eff
1	0.93	7	0.72	13	0.88	19	0.92
2	0.87	8	0.92	14	0.87	20	0.80
3	0.90	9	0.75	15	0.90	21	0.93
4	0.91	10	0.76	16	0.88	22	0.91
5	0.90	11	0.60	17	0.92	23	0.92
6	0.91	12	0.93	18	0.88	24	0.89

The results can be cross-checked with the single fibre efficiencies. The probability to observe a signal in at least one of the two fibres ε_2 can be predicted from the measured single-fibre detection efficiency ε_1.

$$\varepsilon_2 = 1 - (1 - \varepsilon_1)^2$$

These predicted values vary typically 0.86 ± 0.08 (see Table 7.3) in agreement with the measured 0.84 ± 0.05.

With the same ansatz the efficiencies for three fibres have been calculated. These results are summarized in Fig. 7.7. The predicted values are overall 0.95 ± 0.05 and if we skip the fibres considered to be broken it even reaches 0.97 ± 0.01.

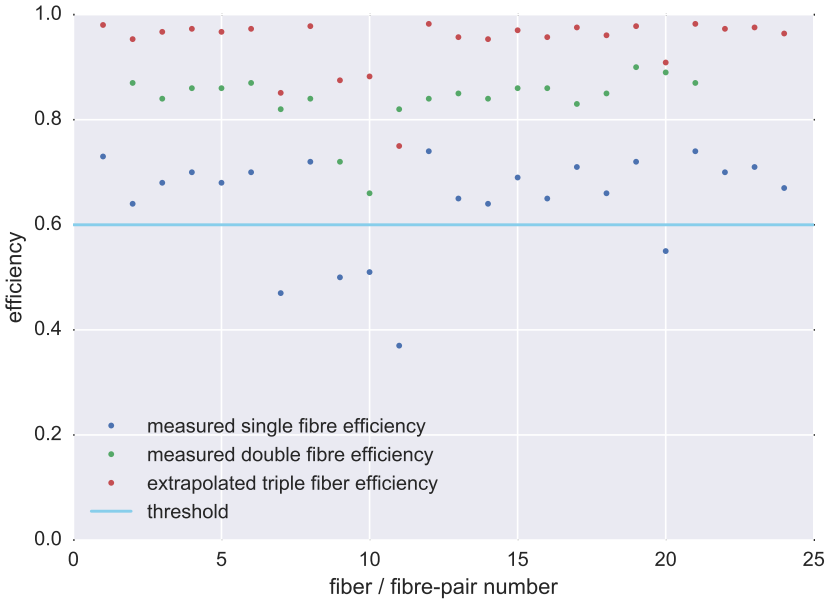

FIG. 7.7 – Cluster efficiency for electrons. The blue line highlights the threshold where the fibres are considered broken or where the coupling to the sensor was bad.